

A THEORY OF MODULATIONAL DIFFUSION

B.V. CHIRIKOV[†], M.A. LIEBERMAN[‡], D.L. SHEPELYANSKY[†] and F.M. VIVALDI^{§*}

[†]*Institute of Nuclear Physics 630090 Novosibirsk, USSR*

[‡]*Dept. of Electrical Engineering and Computer Sciences, University of California Berkeley, CA 94720, USA*

[§]*School of Physics, Georgia Institute of Technology Atlanta, GA 30332, USA*

Received 21 December 1983

Revised 15 September 1984

Modulational diffusion, a weak instability that frequently occurs in many-dimensional, nonlinear Hamiltonian systems, is studied both analytically and numerically. Modulational diffusion arises when an oscillation in one of the degrees of freedom is phase modulated at a slow driving frequency, producing a “modulational layer” of overlapping resonances in phase spaces. Because the motion within this layer is chaotic, any coupling to the oscillation of another degree of freedom produces a long-time diffusion of its associated action along the layer. The diffusion rate for this process is evaluated analytically, and is compared with numerical calculations for a model, two-degree-of-freedom, nonautonomous Hamiltonian. The diffusion coefficient is found to vary in a series of descending steps as the frequency difference between the two oscillators is increased. Good agreement between analytical and numerical results has been obtained over many orders of magnitude in the diffusion coefficient.

1. Introduction

In 1892 Henri Poincaré regarded the problem of studying the motions generated by the Hamiltonian

$$H(\mathbf{I}, \boldsymbol{\theta}, t) = H_0(\mathbf{I}) + \mu H_1(\mathbf{I}, \boldsymbol{\theta}, t); \quad \mu \ll 1, \quad (1.1)$$

as “the fundamental problem of dynamics” [1]. Here the unperturbed Hamiltonian H_0 is integrable depending on the action variables $\mathbf{I} = (I_1, \dots, I_N)$ alone, and μH_1 is a small perturbation which is periodic in the angle variables $\boldsymbol{\theta} = (\theta_1, \dots, \theta_N)$ as well as in time t , with periods 2π and $2\pi/\Omega$, respectively. Some crucial aspects of this problem are still not completely solved, despite the enormous progress made in recent years. For instance, we can regard the Hamiltonian H_0 as describing some bounded oscillations, and ask whether all solutions of the perturbed system are

still bounded. This problem of long-time prediction in many-dimensional Hamiltonian systems, which was originally formulated in the field of celestial mechanics, has in recent times become important in many other branches of physics. As an example, we note the problem of stability of heavy particles (protons and antiprotons) in storage rings. Indeed even in the simplest models of such dynamical processes, both multidimensionality and extremely long time scales must be taken into account (see, e.g., [6]).

One phenomenon relevant to the stability problem in Hamiltonian systems with more than two degrees of freedom is the well-known *Arnold diffusion* [2–7]. Here we shall analyse another source of instability which also seems to be of a very general nature, and which is related to the presence of a slow modulation. When an oscillation in one of the degrees of freedom is phase or frequency modulated at a slow driving frequency, then a set of closely spaced resonances (multiplet) is formed about the oscillation frequency. Above a critical perturbation strength, the multiplet resonances

*Now at Department of Applied Mathematics, Queen Mary College, University of London, Mile End Road, London E1 4NS, England.

overlap [4], producing a relatively broad region of phase space which supports chaotic motion (modulational layer). If these stochastic oscillations are coupled to another degree of freedom, the corresponding dynamical variables become themselves subject to a random evolution. This phenomenon manifests itself as long-time diffusion along the modulational layer (*modulational diffusion* [7–11]). Since these layers in many-degrees-of-freedom non-autonomous systems form a set which in general extends to infinity, this process can completely alter the character of the motions over long times, and even yield unbounded orbits.

The modulational diffusion can be regarded as representative of a larger class of dynamical instabilities, sometimes referred to as “thick layer diffusion” [5]. This terminology is intended to characterize motion along the broad stochastic domains generated by the overlap of several resonances closely situated in the system phase space. A thick layer diffusion differs from Arnold diffusion both in the structure and in the size of the stochastic components involved. Indeed, Arnold diffusion takes place within the narrow stochastic domains (thin layers) which unavoidably appear in the vicinity of separatrices of nonlinear resonances under the effect of arbitrary perturbation. Since thin layers exist for any perturbation strength, so does the Arnold diffusion. In contrast, a thick layer can exist only in some suitable parameter range, so that the same condition will determine the onset of the associated diffusion. We remark that even though these two classes of phenomena share a roughly similar exponential dependence of the diffusion rate on some system parameters, the average rate of thick layer diffusion is generally much larger than that of Arnold diffusion.

A qualitative description of the modulation diffusion, including some semi-empirical estimates of the diffusion rate, was given in ref. 9. In ref. 7 the first analytical theory of this phenomenon was developed. In this work we continue the approach taken in ref. 7 to improve the theory and to achieve a better agreement with numerical simulations. The validity of our approximation scheme is

then verified via numerical calculations on a simple model. Our results are also applicable to a broader class of systems having sufficiently homogeneous thick layers.

2. Formulation of the problem

As a model for modulational diffusion, we consider the Hamiltonian [9]

$$H = \frac{I_1^2}{2} + \frac{I_2^2}{2} - \epsilon \cos(\theta_1 + \lambda \sin \Omega t) - \mu \cos(\theta_1 - \theta_2), \quad (2.1)$$

consisting of the unperturbed part $H_0 = I_1^2/2 + I_2^2/2$, and of two additional terms which comprise the perturbation. Specifically, oscillator 1 is phase modulated with amplitude λ at the slow modulation frequency Ω , and it is coupled to oscillator 2 with coupling strength μ . In order to simplify the calculations, in what follows we shall assume $\epsilon \gg \mu$, so that we can regard the 1-motion as independent of the 2-motion. Expanding the third term in the RHS of (2.1) in Fourier series, we arrive at a Hamiltonian which displays explicitly a set of primary resonances

$$H^{(1)} = \frac{I_1^2}{2} - \epsilon \sum_{n=-\infty}^{\infty} J_n(\lambda) \cos(\theta_1 + n\Omega t). \quad (2.2)$$

For sufficiently large λ , the Bessel functions $J_n(\lambda)$ have significant amplitudes only when $|n| \leq \lambda$, and fall off faster than exponentially for larger indices. This fact ensures the existence of quasi-periodic motion (invariant tori) with sufficiently high frequency $\omega_1 = \partial H^{(1)}/\partial I_1$, and therefore the 1-motion alone is bounded for all times. At the same time the system parameters can be adjusted in such a way as to induce the simultaneous overlap of all resonances with $|n| \leq \lambda$, resulting in the formation of a single layer of half-width $\Delta\omega = M\Omega \approx \lambda\Omega$ centered about the value $\omega_1 = 0$. Here we have introduced the new parameter $M = \Delta\omega/\Omega$ which measures the effective number of resonances

within the layer. This is necessary since M is often somewhat larger than λ (cf. section 6). To describe the resonance overlap, it is convenient to introduce the so-called overlap parameter s , defined as the ratio between the sum of the half-widths (ΔI_1) for the two adjacent resonances and their relative spacing (δI_1) [4]. The critical parameter is then found to correspond to the value $s_{\text{crit}} \approx 2/\pi$ [4], also denoted as the “two-thirds rule” [7]. Applying this criterion, and approximating the amplitude of the Bessel functions by their rms value $(\pi\lambda)^{-1/2}$ one obtains from (2.2) the half-width $\Delta I_1 \approx 2\varepsilon^{1/2}(\pi\lambda)^{-1/4}$, the spacing $\delta I_1 \approx \delta\omega_1/(d\omega_1/dI_1) = \Omega$, and the overlap condition takes the simple form [9]

$$\frac{\pi^2 s^2}{4} \approx \frac{23\varepsilon}{\Omega^2 \sqrt{\lambda}} \geq 1. \quad (2.3)$$

According to this expression, resonance overlap will typically occur when the modulation frequency is sufficiently small. We remark however that the limit $\Omega \rightarrow 0$ must be taken with some care. To this end let us first change variables using the generating function

$$F(\bar{I}, \theta_1, t) = (\bar{I} - \lambda\Omega \cos \Omega t) \cdot (\theta_1 + \lambda \sin \Omega t), \quad (2.4)$$

where the new Hamiltonian $K = H^{(1)} + \partial F/\partial t$,

$$K = \frac{\bar{I}^2}{2} - \varepsilon \cos \bar{\theta} + \bar{\theta} \lambda \Omega^2 \sin \xi - \frac{\lambda^2 \Omega^2}{2} \cos^2 \xi, \quad (2.5)$$

now depends on the “slow time” variable $\xi = \Omega t$. By inspecting the “potential energy” $u(\bar{\theta}) = -\varepsilon \cos \bar{\theta} + \bar{\theta} \lambda \Omega^2 \sin \xi$ for any fixed ξ , we note that as long as

$$V \equiv \frac{\lambda \Omega^2}{\varepsilon} < 1, \quad (2.6)$$

there is always a stable domain centered about an elliptic “fixed point” $\bar{\theta}_0$, where $\varepsilon \sin \bar{\theta}_0 = -\lambda \Omega^2 \sin \xi$, and $\varepsilon \cos \bar{\theta}_0 > 0$. In other words when (2.6) is satisfied, some phase points experience a

stable local environment, although slowly changing with time. Under this adiabatic perturbation, the local action $\bar{I}' = \bar{I}'(\xi)$ about the fixed point can be shown to be bounded by KAM tori forever [12]. In the original variables, this condition corresponds to the appearance of a periodically oscillating stable region within the modulational layer. This phenomenon is known as “trapping” [13, 14]. We note that the relative size of this stable domain is small provided that the modulational layer half-width $\lambda\Omega$ is large compared to the trapping resonance half-width $2\sqrt{\varepsilon}$. This yields the condition

$$\left(\frac{\lambda\Omega}{2\sqrt{\varepsilon}} \right)^2 \gg 1 \quad (2.7)$$

for the absence of trapping. As $\Omega \rightarrow 0$, one should consider two different cases, depending on whether λ or the product $\lambda\Omega$ (i.e., the layer width) is kept constant. In the former case the inequality (2.7) is always violated, and all multiplet resonances merge together to form a single resonance, surrounded by a thin stochastic layer. In the latter case, the condition (2.7) can be satisfied for a suitable choice of the parameter values. Even though the stochastic trajectories still spread over most of the layer, some statistical properties of the motion change considerably. For example, the diffusion rate across the layer has been shown to vary as Ω^3 [14]. Note that in this case the limit $\Omega \rightarrow 0$ is singular in the sense that for $\Omega = 0$ only one resonance ($\omega_1 = -\lambda\Omega$) remains, and the motion (2.2) is perfectly regular.

The following analysis will be developed assuming not only the overlap condition (2.3), but also the absence of trapping. The influence of the latter phenomenon on modulational diffusion will be briefly discussed in section 7.

Let us now consider the full system (2.1). The geometrical structure of the associated phase space is most easily illustrated in the frequency plane $(\omega_1, \omega_2) = (\partial H_0/\partial I_1, \partial H_0/\partial I_2)$, which in our case coincides with the action plane (I_1, I_2) . Here the layer is represented as an unbounded strip (fig. 1). When the two oscillators are uncoupled ($\mu = 0$) I_2

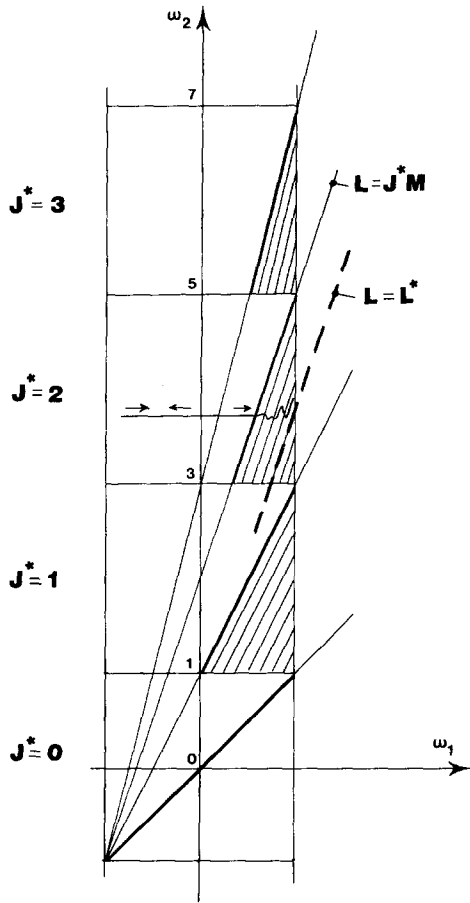


Fig. 1. Geometrical structure of a modulational layer (unmodulated driving resonance, $q = 1$).

is invariant, and therefore motion along the layer is forbidden. The global stability of the full system then follows directly from that of the reduced system (2.2).

Now let $\mu \neq 0$. (Recall, however, that $\mu \ll \epsilon$). The motion in the 2-direction is governed by the time-dependent Hamiltonian

$$H^{(2)} = \frac{I_2^2}{2} - \mu \cos(\theta_1(t) - \theta_2). \tag{2.8}$$

When the 1-motion takes place within the modulational layer, (2.8) describes a nonlinear oscillator (pendulum) driven by the external *random* motion $\theta_1(t)$, obtained by solving the motion for (2.2).

This accounts for the random evolution of phase points in the I_2 direction. In particular, the time evolution of a stochastic orbit could cause action points to explore the entire layer domain. The resonance ($\omega_1 \approx \omega_2$) appearing in (2.8) is generally referred to as the “driving resonance” since it is responsible for driving the diffusion along the modulational layer. The problem is to determine the rate at which the action I_2 (or any function of it) diffuses. The diffusion coefficient is defined as

$$D(I_2) = \frac{\langle [\Delta I_2(T)]^2 \rangle}{2T}, \tag{2.9a}$$

$$\Delta I_2(T) = - \int_{-T}^T dt' \frac{\partial H^{(2)}}{\partial \theta_2}, \tag{2.9b}$$

where the average is over an appropriate ensemble of initial phase points (see section 3), and where T is much larger than the diffusion time across the modulational layer but much less than that along the layer. Evaluation of (2.9) in some perturbation scheme would in principle require knowledge of the full set of resonances of the system (2.1). However, we will show that the long-range diffusion is essentially supported by a selected set of secondary resonances. Due to this simplification the diffusion coefficient can be evaluated by means of first-order canonical perturbation theory.

3. Diffusion rate

We now derive an expression for the diffusion rate, and in particular we show that $D(I_2)$ varies as a series of descending steps as I_2 increases from zero, to give an overall exponential dependence, in agreement with some originally puzzling numerical results [7] (see fig. 5). The time evolution of I_2 is determined by Hamilton’s equation (cf. (2.1))

$$\dot{I}_2 = \mu \sin(q\theta_1 - \theta_2), \tag{3.1}$$

which has been slightly generalized by introducing the additional parameter q which is relevant to the case of higher-harmonic driving resonances. In order to calculate D as in (2.9) we need an explicit

expression for the phase variation $\Phi = q\theta_1(t) - \theta_2(t)$ in (3.1). Since we are interested only in the local behavior (in I_2), we let $\mu = 0$ in (2.8) to obtain

$$\theta_2 = \omega_2 t - \theta_0. \quad (3.2)$$

On the other hand, the 1-motion must incorporate the effect of the modulation at first order in ε , since $\varepsilon \gg \mu$, so we write

$$H_0^{(1)} = \frac{I_1^2}{2}, \quad (3.3a)$$

$$H_1^{(1)} = -\varepsilon \sum_{n=-\infty}^{\infty} J_n(\lambda) \cos(\theta_1 + n\Omega t), \quad (3.3b)$$

and decompose I_1 and θ_1 into zeroth and first order parts

$$I_1 = I_{10} + I_{11}; \quad \theta_1 = \theta_{10} + \theta_{11}. \quad (3.4)$$

At zeroth order $I_{10} = I_0 = \text{const}$ and $\theta_{10} = I_0 t + \theta_{00}$; $\Phi_0 = q\theta_{00} + \theta_0$. In first order

$$\begin{aligned} \dot{I}_{11} &= -\frac{\partial H_1^{(1)}}{\partial \theta_1} \\ &= -\varepsilon \sum_{n=-\infty}^{\infty} J_n(\lambda) \sin(\theta_{10} + n\Omega t), \end{aligned} \quad (3.5a)$$

$$\dot{\theta}_{11} = I_{11}. \quad (3.5b)$$

Letting $\theta_{10} = I_0 t + \theta_{00}$ in (3.5a) and integrating first (3.5a) and then (3.5b) over time, we obtain

$$\begin{aligned} \theta_1(t) &= I_0 t + \varepsilon \sum_{n=-\infty}^{\infty} \frac{J_n(\lambda)}{(I_0 + n\Omega)^2} \sin[(I_0 + n\Omega)t] \\ &\quad + \theta_{00}. \end{aligned} \quad (3.6)$$

Inserting (3.6) into (3.1) and expanding again, we obtain

$$\begin{aligned} \sin \Phi(t) &= \sum_j \left\{ \prod_{m=-\infty}^{\infty} A(m, I_0) \right\} \\ &\quad \times \sin \left\{ \left[\left(\sum_{n=-\infty}^{\infty} j_n + q \right) I_0 \right. \right. \\ &\quad \left. \left. + \sum_{n=-\infty}^{\infty} j_n n \Omega - \omega_2 \right] t + \Phi_0 \right\}, \end{aligned} \quad (3.7)$$

where $j = (\dots, j_{-1}, j_0, j_1, \dots)$ with each j_m an integer and

$$A(m, I_0) = J_{j_m} \left[\frac{q\varepsilon J_m(\lambda)}{(I_0 + m\Omega)^2} \right]. \quad (3.8)$$

After defining

$$J = \sum_{n=-\infty}^{\infty} j_n; \quad L = \sum_{n=-\infty}^{\infty} j_n n, \quad (3.9)$$

we rewrite the sum (3.7) as follows:

$$\begin{aligned} \sin \Phi(t) &= \sum_{J, L=-\infty}^{\infty} B(J, L, I_0) \\ &\quad \times \sin \{ [(J + q)I_0 + L\Omega - \omega_2] t + \Phi_0 \} \end{aligned} \quad (3.10a)$$

with

$$B(J, L, I_0) = \sum_{J, L=\text{const}} \left[\prod_{m=-\infty}^{\infty} A(m, I_0) \right]. \quad (3.10b)$$

The sum in the RHS of (3.10b) is taken over all combinations of j yielding J and L constant. This expression shows that the first-order interaction between the primary resonances in (2.2) and in (2.8) generates an infinite array of secondary driving resonances, whose amplitudes depend on I_0 . We know that over long times the system samples all values $|I_0| < \Delta\omega$ within the modulational layer, so we shall average over that domain in what follows.

The diffusion coefficient (2.9) becomes

$$\begin{aligned} D(\omega_2) &\approx \frac{\mu^2}{2\Delta\omega} \frac{1}{2T} \left\langle \int_{-\Delta\omega}^{\Delta\omega} dI_0 \int_{-T}^T dt' \sin \Phi(t') \right. \\ &\quad \left. \times \int_{-T}^T dt'' \sin \Phi(t'') \right\rangle_{\Phi_0}, \end{aligned} \quad (3.11)$$

where both integrands are given by (3.7). We first perform the t'' integration to obtain

$$\begin{aligned} \int dt'' \sin \Phi(t'') &= \sum_{J, L=-\infty}^{\infty} B(J, L, I_0) \\ &\quad \times \frac{2\pi \sin \Phi_0}{J + q} \delta \left(I_0 - \frac{\omega_2 - L\Omega}{J + q} \right). \end{aligned} \quad (3.12)$$

Then we substitute (3.12) into (3.11) and perform the I_0 integration. The δ -function in (3.12) determines the condition

$$I_0 = \frac{\omega_2 - L\Omega}{J + q}. \quad (3.13)$$

Due to (3.13) the integrand in (3.11) is independent of t' , so that the t' integral can be performed immediately. We obtain

$$D(\omega_2) \approx \frac{\pi\mu^2}{\Delta\omega} \sum_{J, L=-\infty}^{\infty} B^2(J, L) \frac{\langle \sin^2 \Phi_0 \rangle_{\Phi_0}}{J + q}. \quad (3.14)$$

From (3.8), (3.10b) and (3.13) the amplitudes $B(J, L)$ are

$$B(J, L) = \sum_{J, L=\text{const}} \left\{ \prod_{m=-\infty}^{\infty} J_{j_m} \left\{ \frac{q\epsilon}{(\Delta\omega)^2} \right. \right. \\ \left. \left. \times \frac{J_m(\lambda)(J+q)^2}{\left[\alpha - \frac{1}{M} [L - m(J+q)] \right]^2} \right\} \right\}, \quad (3.15)$$

where the dimensionless variable

$$\alpha = \frac{\omega_2}{\Delta\omega} \quad (3.16)$$

measures the displacement in the 2-direction in unit of the layer half-width. After averaging over Φ_0 , (3.14) becomes

$$D(\alpha) \approx \frac{\pi\mu^2}{2\Delta\omega} \sum_{J, L=-\infty}^{\infty} \frac{B^2(J, L)}{J + q}, \quad (3.17)$$

which is exact to first order in ϵ , and therefore it includes the contribution of all primary and secondary driving resonances.

4. Dominant terms

The resonances which determine the diffusion rate (3.17) correspond to resonance lines in the

frequency plane with equations (cf. (3.10a)).

$$\omega_2 = (J + q)\omega_1 + L\Omega. \quad (4.1)$$

Because of the motion across the layer, the phase points intersect these lines repeatedly, receiving a small impulse in the 2-direction at each crossing (fig. 1). The magnitude of this displacement is determined by the phase and the amplitude of the resonant term involved. Since the 1-motion is bounded, for any given α not all resonances can be crossed. In addition many of the resonances that are actually crossed have negligible amplitude, and therefore the range of summation in (3.17) can be considerably restricted. To this end we first note that the argument of the Bessel function J_{j_m} is typically small ($\epsilon \ll 1$, see (3.8)), so that they are accurately approximated by the asymptotic expression

$$J_j(\chi) \approx \frac{1}{j!} \left(\frac{\chi}{2} \right)^j; \quad \chi \ll 1, \quad j \geq 0. \quad (4.2)$$

From (4.2) and recalling that $J_m(\lambda)$ in (3.15) is exponentially small when $|m| > M$ (cf. section 2), we can restrict ourselves to the domain

$$|m| \leq M. \quad (4.3)$$

We shall sum (3.17) in the range (4.3), regrouping the terms with constant J . Using (4.2) in (3.17) and replacing $J_m(\lambda)$ with the asymptotic ($\lambda \gg 1$, $|n| \leq \lambda$) formula

$$J_m(\lambda) \approx \sqrt{\frac{2}{\pi\lambda}} \sin\left(\lambda - \frac{\pi}{2}m + \frac{\pi}{4}\right), \quad (4.4)$$

the normalized diffusion rate $D_R = D\Delta\omega/\mu^2$ then becomes

$$D_R(\alpha) \approx \sum_{J=-\infty}^{\infty} D_J(\alpha), \quad (4.5a)$$

with

$$\begin{aligned}
 D_J(\alpha) &= \frac{\pi}{2} |J + q|^{4|J|-1} \left[\frac{q\epsilon}{\sqrt{2\pi\lambda} (\Delta\omega)^2} \right]^{2|J|} \\
 &\times \sum_L \left\{ \sum_{J, L = \text{const}} \left\{ \prod_{m=-M}^M (|j_m|!)^{-1} \right. \right. \\
 &\times \left. \left. \left[\alpha - \frac{1}{M} (L - m(J + q)) \right]^{-2|j_m|} \right. \right. \\
 &\times \left. \left. \sin \left(\lambda - \frac{\pi}{2} m + \frac{\pi}{4} \right)^{|j_m|} \right\} \right\}^2, \quad (4.5b)
 \end{aligned}$$

which is valid provided that the denominators in the RHS are not too small. For $J \geq 1$ the dominant terms of (4.5) are readily identified as the ones for which J of the j_m 's are equal to one, while all the remaining j_m 's are equal to zero. Indeed from (4.2) and (4.5) it is seen that negative values of j_m will correspond to an overall exponent for α exceeding J by at least two, while any term containing $j_m > 1$ will be reduced by a factor $(j_m!)$. Thus all these terms can be neglected. With this prescription (3.13) can be rewritten as

$$J = \left(\alpha - \frac{\sum_k n_k}{M} \right) \frac{\Delta\omega}{I_0} - q, \quad (4.6)$$

where the sum $L = \sum_k n_k$ in the RHS now consists of J terms. For any fixed α the dominant term in (4.5b) corresponds to the smallest value $J^*(\alpha)$ of J compatible with (4.3). J^* can be obtained from (4.6) by maximizing both L and I_0 . The largest allowed value L_{\max} of L is given by the expression

$$L_{\max} = \sum_{k=0}^{J-1} (M - k) = J \left(M - \frac{J-1}{2} \right). \quad (4.7)$$

Since $M \gg 1$, for J not too large, we can write $L_{\max} \approx JM$. Replacing this expression in (4.6) with $I_0 = \Delta\omega$ we obtain

$$J^* = J^*(\alpha) = \left[\frac{1}{2} (\alpha - q) \right]_1. \quad (4.8)$$

where $[x]_1$ denotes the smallest integer larger than

x . Therefore $J^*(\alpha)$ is an increasing step-function of α , with discontinuities at the value $\alpha_n = 2n + q$, $n = 0, 1, 2, \dots$. Within each interval $\Delta\alpha_n = [\alpha_n, \alpha_{n+1}]$ the diffusion rate (4.4) is essentially determined by the single term D_{J^*} , and therefore the diffusion coefficient will be discontinuous at the same values α_n . In particular, due to (4.2), $D_R(\alpha)$ will exhibit a sequence of descending steps (hereafter referred to as "plateaus").

To complete our approximation scheme, we must still retain from the resonances (4.1) with $J = J^*$, only the ones that can be crossed. These must satisfy the condition

$$\begin{aligned}
 L^* &\equiv \left[\alpha - (J^* + q) \right]_1 M \leq L \\
 &= \sum_k n_k \leq \left[\alpha + (J^* + q) \right]_1 M, \quad (4.9)
 \end{aligned}$$

which is readily obtained from (4.1) by letting $\omega_1 = \mp \Delta\omega$ respectively. Since the upper bound of (4.9) is always larger than $L^* = J^*M$, we can replace (4.9) by the more restrictive condition

$$L^* \leq L \leq J^*M. \quad (4.10)$$

Taking into account (4.3) and (4.10), the partial contributions D_{J^*} (cf. (4.5)) can be written as

$$\begin{aligned}
 D_{J^*}(\alpha) &= K(J^*) \\
 &\times \sum_{L=L^*}^{J^*M} \left\{ \sum_{n_1 + \dots + n_{J^*} = L} \left\{ \prod_{i=1}^{J^*} \Delta(\alpha, n_i) \right\} \right\}^2, \quad (4.11)
 \end{aligned}$$

where

$$K(J^*) = \frac{\pi}{2} |J^* + q|^{4|J^*|-1} \left[\frac{q\epsilon}{\sqrt{2\pi\lambda} (\Delta\omega)^2} \right]^{2|J^*|}, \quad (4.12a)$$

$$\Delta(\alpha, n_i) = \frac{\sin \left(\lambda - \frac{\pi}{2} n_i + \frac{\pi}{4} \right)}{\left\{ \alpha - \frac{1}{M} [L - n_i (J^* + q)] \right\}^2}, \quad (4.12b)$$

and

$$-M \leq n_1 < n_2 < \dots < n_{J^*} \leq M. \tag{4.13}$$

The resonance lines with $J = J^*$, and L satisfying (4.10) are displayed in fig. 1. They define triangular-shaped regions within the modulational layer (interaction regions) where the diffusion process is originated, as a consequence of resonance crossing. We remark that this geometrical structure is common to any sufficiently homogeneous thick layer, formed by the overlap of a large number of resonances with comparable amplitude, spacings and directions. For this reason the estimate (4.11) can be viewed as typical of thick layer diffusion, provided that the Bessel functions are replaced by the appropriate resonance amplitudes.

The sum (4.11) can be explicitly evaluated for small J . For $J^* = 0$ (or $\alpha \in [-q, q]$) we have directly from (4.5b) (the product within the braces in (4.11) collapses to unity)

$$D_0 \approx \frac{\pi}{2q}, \tag{4.14}$$

that is the primary plateau is flat. Indeed in this domain the diffusion is supported by the primary driving resonance, whose amplitude is constant. For $J^* = 1$ (4.11) takes on the simple form

$$D_J(\alpha) = K(J)(J!)^{-2} \sum_{n=L^*/J}^M \Delta(\alpha, n)^{-4J}, \tag{4.15}$$

where $\sum_k n_k = n_i$ in (4.12b) and the J -dependence has been written out explicitly, in preparation for future use (see section 6). Here, however, we consider only $J = 1$. After transforming (4.15) into an integral (and $J_m(\lambda)$ in (4.4) replaced by its rms value $(\pi\lambda)^{-1/2}$) we obtain

$$D_J(\alpha) = K'(J) \frac{M}{(4J-1)q} [f(\alpha) + g(\alpha)], \tag{4.16}$$

with

$$K'(J) = \frac{\pi}{2} |J + q|^{4|J|-1} \left[\frac{q\varepsilon}{2\sqrt{\pi\lambda}(\Delta\omega)^2} \right]^{2|J|}, \tag{4.17a}$$

$$f(\alpha) = [(\alpha - q)(J + q)/J]^{1-4|J|}, \tag{4.17b}$$

$$g(\alpha) = -(\alpha + q)^{1-4|J|}, \tag{4.17c}$$

which is invalid at and near $\alpha = q$, where the argument of the Bessel functions diverges and (4.2) no longer holds. This singularity corresponds to a sudden drop in the diffusion rate at the end of the primary plateau ("precipice" [9], see also section 6).

5. Modulated driving resonance

Of considerable interest in practical application is the more general case in which the driving perturbation is also modulated. In this case the diffusion originates near the intersection of two multiplets. As a model for this process we study the following example

$$\dot{J}_2 = \mu \sin(q\theta_1 - \theta_2 + \lambda \sin \Omega t) \equiv \mu \sin \Phi, \tag{5.1}$$

that is we have modified (3.1) by introducing a modulation in the phase of the coupling term. For simplicity, both amplitude and frequency of the modulation have been assumed to be identical to those of the first degree of freedom. The generalization of the following analysis to different values of these parameters is straightforward. Expanding the RHS of (5.1) as in (3.7) we obtain

$$\begin{aligned} \sin \Phi(t) = & \sum_{J,p} \left\{ \prod_{m=-\infty}^{\infty} A(m, I_0) \right\} J_p(\lambda) \\ & \times \sin \left\{ \left[\left(\sum_{n=-\infty}^{\infty} j_n + q \right) I_0 \right. \right. \\ & \left. \left. + \left(\sum_{n=-\infty}^{\infty} j_n n + p \right) \Omega - \omega_2 \right] t + \Phi_0 \right\}, \end{aligned} \tag{5.2}$$

where the $A(m, I_0)$ are given by (3.8). Following the procedure developed in section 4 with $J_p(\lambda) \approx (\pi\lambda)^{-1/2}$, the normalized diffusion rate becomes (cf. (4.4-5))

$$D_R(\alpha) = \frac{1}{2\lambda} \sum_{J, L=-\infty}^{\infty} \frac{B^2(J, L)}{J+q}, \quad (5.3)$$

where

$$B(J, L) = \sum_{J, L=\text{const}} \left\{ \prod_{m=-\infty}^{\infty} J_{j_m} \left(\frac{q\epsilon}{(\Delta\omega)^2} \frac{J_m(\lambda)(J+q)^2}{\left[\alpha - \frac{1}{M} [L - m(J+q)] \right]^2} \right) \right\}, \quad (5.4)$$

with

$$J = \sum_n j_n; \quad L = L(p) = \sum_k n_k + p. \quad (5.5)$$

Eq. (4.6) now becomes

$$J = \left(\alpha - \frac{\sum_k n_k + p}{M} \right) \frac{\Delta\omega}{I_0} - q, \quad (5.6)$$

which, for any given α , is minimized by letting $I_0 = \Delta\omega$, $\sum_k n_k = JM$ and $p = M$, to give

$$J^* = J^*(\alpha) = \left[\frac{1}{2}(\alpha - q - 1) \right]_1, \quad (5.7)$$

so that the primary plateau is broader than that of the unmodulated case, and all secondary plateaus are shifted (fig. 2). For $J = J^*$ the resonances crossed must now satisfy the condition

$$L^* \equiv \left[\alpha - (J^* + q) \right]_1 M \leq L \leq (J^* + 1)M \quad (5.8)$$

and therefore the diffusion rate becomes

$$D_{J^*}(\alpha) = K(J^*) \sum_{L=L^*}^{J^*M} \left\{ \sum_{n_1 + \dots + n_{J^*} + p = L} \prod_{i=1}^{J^*} \Delta(\alpha, n_i, p) \right\}^2, \quad (5.9)$$

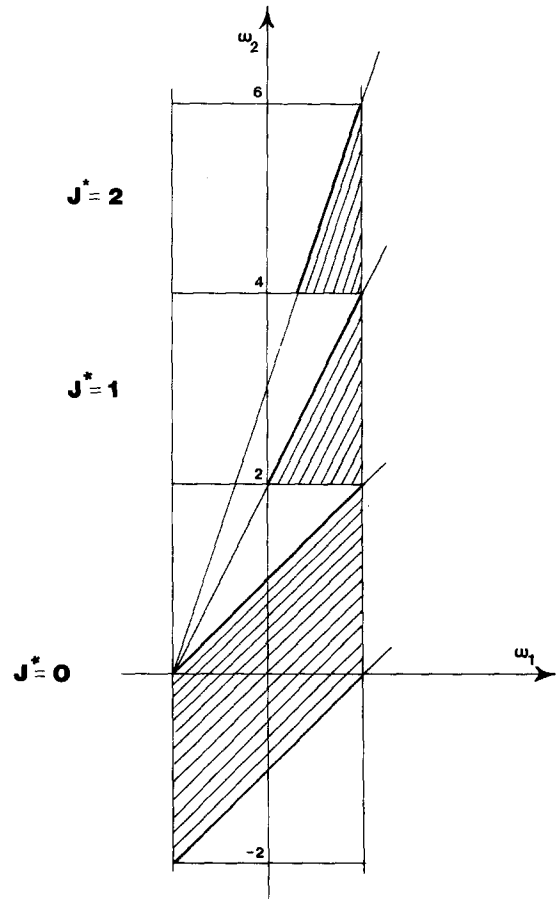


Fig. 2. Geometrical structure of a modulational layer (modulated driving resonance, $q = 1$).

where

$$K(J^*) = \frac{1}{2\lambda} |J^* + q|^{4|J^*|-1} \left[\frac{q\epsilon}{\sqrt{2\pi\lambda} (\Delta\omega)^2} \right]^{2|J^*|}, \quad (5.10a)$$

$$\Delta(\alpha, n_i, p) = \frac{\sin\left(\lambda - \frac{\pi}{2}n_i + \frac{\pi}{4}\right)}{\left\{ \alpha - \frac{1}{M} [L(p) - n_i(J^* + q)] \right\}^2}. \quad (5.10b)$$

Again the sum (5.9) can be explicitly evaluated for small J . When $J^* = 0$, or $|\alpha| < q + 1$, all j_m 's

are zero so that (5.8) reads

$$(\alpha - q)M \leq p \leq M, \quad (5.11)$$

that is the diffusion coefficient is the sum of $M(1 + q - \alpha)$ identical terms or

$$D_0(\alpha) \approx \frac{M}{2\lambda q} (1 + q - \alpha). \quad (5.12)$$

On the first plateau ($J^* = 1$ or $\alpha \in [1 + q, 3 + q]$) eq. (5.9) becomes

$$D_J(\alpha) = K(J)(|J|!)^{-2} \times \sum_{n=\frac{L^*-M}{J}}^M \sum_{p=L+Jn}^M \Delta(\alpha, n, p)^{-4|J|}, \quad (5.13)$$

where we have again included the J -dependence explicitly. Evaluation of (5.13) now yields

$$D_J(\alpha) = K'(J) \frac{M^2}{(|J|!)^2 (4|J| - 1)(4|J| - 2)} \times [f(\alpha) + g(\alpha) + h], \quad (5.14)$$

where

$$K'(J) = \frac{1}{2\lambda} |J + q|^{4|J| - 1} \left[\frac{q\epsilon}{2\sqrt{\pi\lambda} (\Delta\omega)^2} \right]^{2|J|}, \quad (5.15a)$$

$$f(\alpha) = \frac{1}{q} \left(\frac{J + q}{J} \right)^{1 - 4|J|} (\alpha - q - 1)^{2 - 4|J|}, \quad (5.15b)$$

$$g(\alpha) = - \frac{(\alpha + q - 1)^{2 - 4|J|}}{q}, \quad (5.15c)$$

$$h = 2[2|J + q|]^{1 - 4|J|}. \quad (5.15d)$$

As before (5.14) is invalid at and near $\alpha = q + 1$ where $f(\alpha)$ diverges.

6. Numerical results

In order to evaluate the accuracy of our approximation scheme we have computed numerically the diffusion rate (2.9) for both the unmodulated and the modulated driving resonance (for numerical techniques see [4, 6, 10]). To increase the efficiency of the computation we have ignored the influence of the 2-motion on the 1-motion, consistent with the assumption $\epsilon \gg \mu$ (cf. section 2). Then the processes described by (3.1) and (5.1) respectively, have been simulated numerically, with the phase θ_1 evolving according to the uncoupled Hamiltonian (2.2), with parameters $\lambda = 10$, $\Omega = 0.01$, $\epsilon = 5 \times 10^{-4}$, and $q = 1$. The corresponding effective layer half-width $\Delta\omega$ has been evaluated via resonance overlap, by taking into account the actual amplitude of the Bessel functions in correspondence to the boundary of the layer. In this way one finds $\Delta\omega = 1.45 \lambda\Omega$ or $M = 14$, in good agreement with a numerical value obtained by computing the equilibrium probability distribution of the action I_1 (fig. 3). In this case the actual layer width exceeds that predicted by the cruder estimate $M = \lambda = 10$ (see section 2) mainly because λ is not large enough.

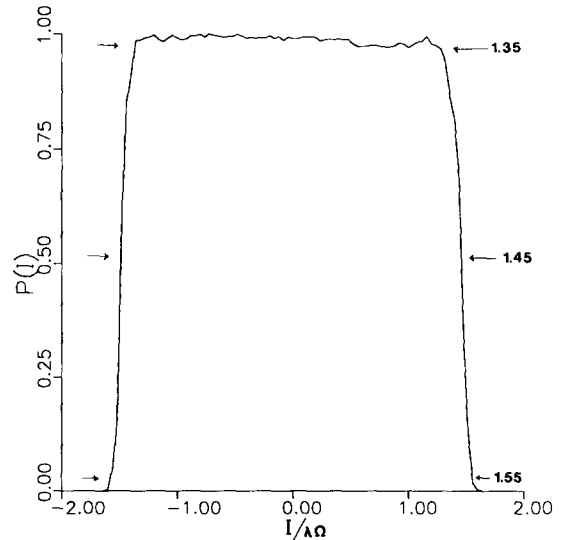


Fig. 3. The layer width: action probability distribution.

In fig. 4 we plot the results for the unmodulated case. The thick solid line represents the analytical expressions (4.14) and (4.16) for $J = 0$ and $J = 1$, respectively, whereas the thin line corresponds to the sum (4.11) evaluated numerically for $J = 1-4$. We have obtained the best fit with the numerical data by letting $\Delta\omega = 1.35\lambda\Omega$ or $M = 13$, which corresponds to the portion of the layer over which the probability distribution is constant (see fig. 3). The small oscillations in the thin line of fig. 4 reflect the presence of the sine function in (4.12b). One sees that the terms we have selected from the first-order expression (3.17) are sufficient to provide an accurate estimate of the diffusion rate, at least in that region of the modulational layer where the diffusion is rapid enough. Beyond the first plateau, (4.11) instead yields a small but significant underestimate of the diffusion coefficient, and

moreover it does not reproduce correctly the dependence on α within each plateau. For this reason it appears that no prediction about the asymptotic ($\alpha \rightarrow \infty$) behaviour of $D(\alpha)$ can be made using the first-order scheme we have developed. A qualitative description of the structure of the tail can nonetheless be derived from the following considerations:

- 1) No secondary plateau is levelled, since the amplitude of all secondary driving resonances decreases as α increases (see (3.15)). In addition, for any given α , the diffusion is driven mainly by the resonances located by the right boundary of the layer (that is with $L = L^*$), whose amplitude is maximal.
- 2) For all plateaus the number of resonances located within the interaction regions decreases with increasing α (see fig. 1).

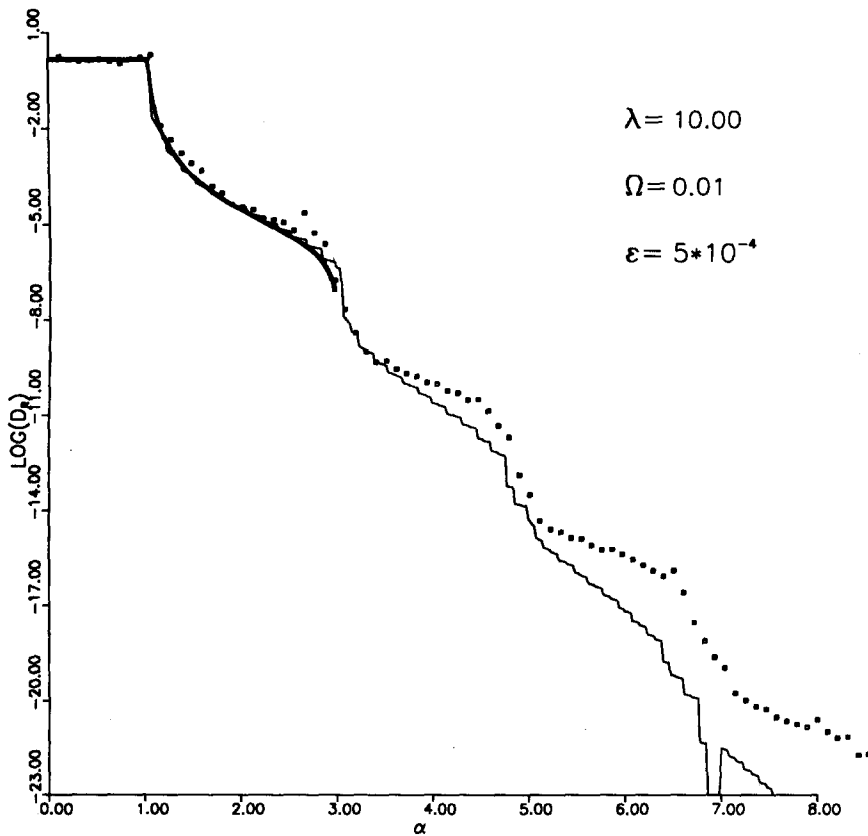


Fig. 4. Normalized diffusion rate. First-order dominant terms.

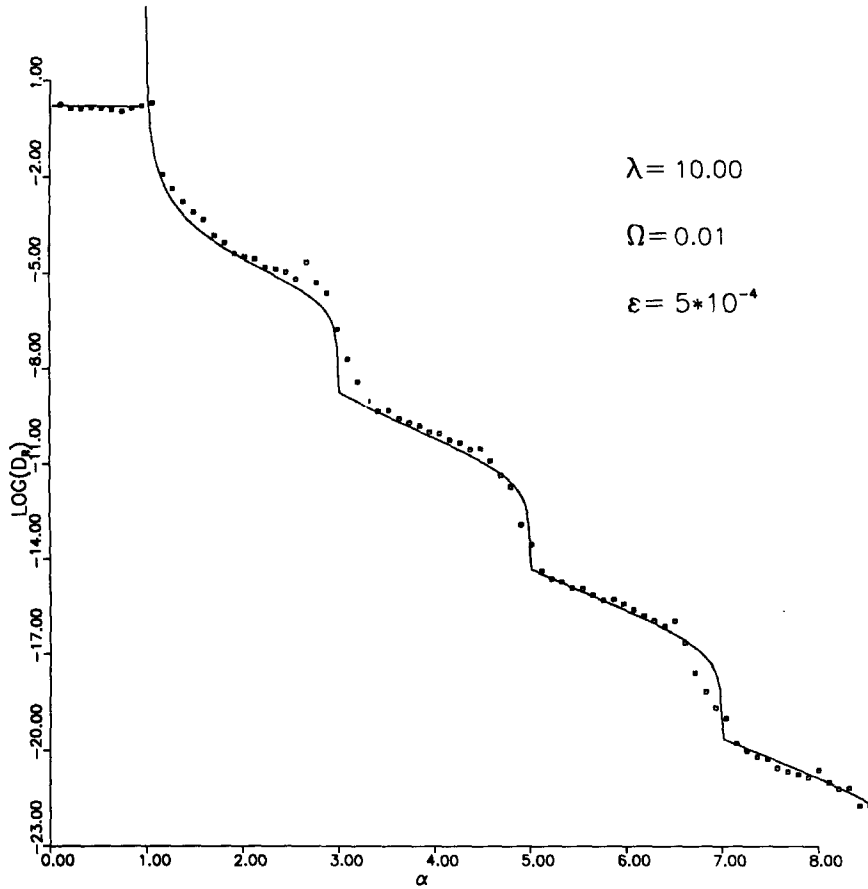


Fig. 5. Scaled diffusion coefficient (unmodulated driving resonance).

Both essential features are accounted for in the estimate (4.16), and therefore the latter can be generalized to the case $|J| > 1$, provided that a fitting parameter $R = R(J)$ (to be determined numerically) is inserted in expression (4.17a) by replacing ϵ with $\epsilon R(J)$. In doing so we intend to fit the numerical data by adjusting the overall perturbation strength. It can be readily seen that for every J the sum (4.16) gives the partial contribution of those terms in (3.7) for which all j_m 's are zero except one. In fig. 5 we display the scaled diffusion rate (4.16) for $J = 1-4$ where the parameter R is found to increase linearly,

$$R(J) \approx 2J - 1. \tag{6.1}$$

The good agreement with the numerical data, not

only in the overall decay rate, but also in the detailed structure of the tail, suggests that the diffusion coefficient may possess self-similar properties. In particular, if (6.1) is assumed valid for all J and the plateau oscillations averaged away, the asymptotic ($\alpha \rightarrow \infty$) decay rate becomes

$$D_R(\alpha) \xrightarrow{\alpha \rightarrow \infty} C(\alpha) e^{B(\alpha-q)} \tag{6.2}$$

where

$$C(\alpha) = \frac{2qM}{\alpha^3} e^{2q-1}, \tag{6.3a}$$

$$B = 1 + \ln \left[\frac{q\epsilon}{(2\Delta\omega)^2 \sqrt{\pi\lambda}} \right]. \tag{6.3b}$$

Expressions (6.2-3) are obtained from (4.16-17) by letting $J = \frac{1}{2}(\alpha - q)$, and then taking the limit $\alpha \rightarrow \infty$. The exponential-type diffusion coefficient we find for modulational diffusion has already been detected in the case of Arnold diffusion [4-6], and it seems to be a distinctive feature of this class of instabilities.

In fig. 6 we plot the expressions (5.12) and (5.14), (for $J = 0$ and $J > 0$, respectively), which correspond to the case of a modulated driving resonance (cf. section 6). As before we have introduced a fitting parameter $R = R(J)$ which is determined numerically as

$$R(J) \approx 2J. \tag{6.4}$$

$R(J)$ is still linear, but now $R(1) = 2$, and there-

fore the expression (5.14) underestimates the diffusion rate. A similar discrepancy can also be seen on the main plateau (fig. 6) where no fitting parameter was introduced. In addition the best fit with the numerical data here corresponds to $M = 12$, slightly smaller than the value employed in the unmodulated case ($M = 13$). In this respect we observe that the effect of the modulation is to subdivide the amplitude of the original driving resonance among the multiplet elements, so that it is conceivable that $J + 1$ terms might contribute significantly also on the J th plateau, and in particular near its far end. Comparison with the previous case reveals that by modulating the driving resonance one can considerably enhance the diffusion coefficient, especially for small α , due to the expansion of the size of the main plateau.

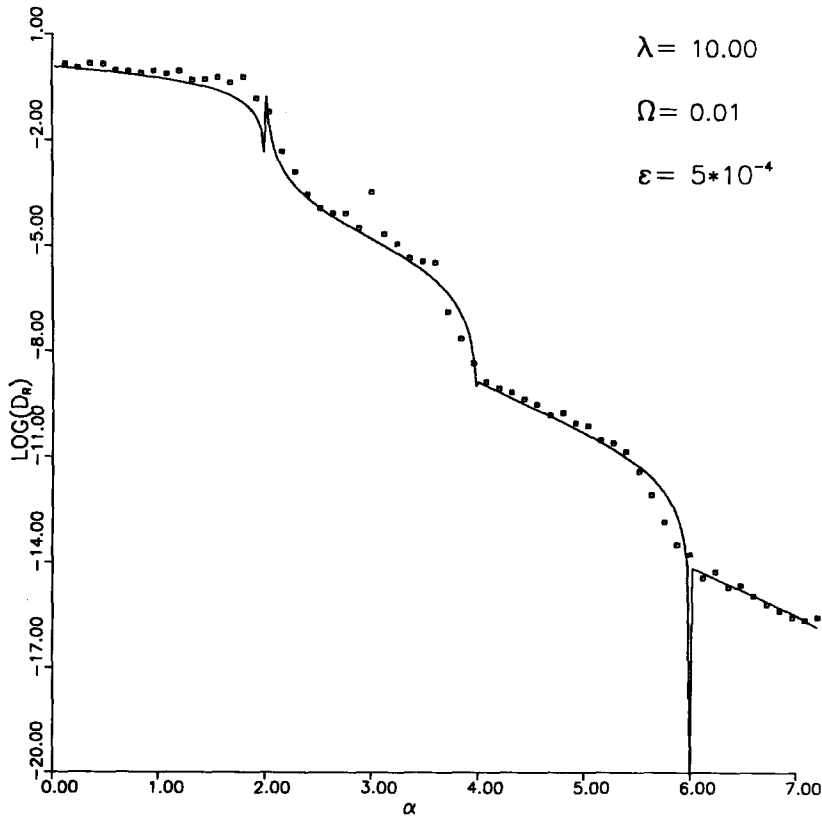


Fig. 6. Scaled diffusion coefficient (modulated driving resonance).

7. Concluding remarks

The derivation of the coefficient of modulational diffusion (3.17) was based on the validity of certain statistical assumptions. Specifically, the phase average appearing in (3.11) was performed assuming a rapid decay of autocorrelations of the dynamical variable $\theta_1 = \theta_1(t)$ associated with the motion across the modulational layer. Such randomization is guaranteed by the simultaneous validity of the inequalities $s > 1$ (overlap) and $V > 1$ (no trapping), respectively (see section 2). It should be stressed however, that if the system is in the trapping regime ($V < 1$), phase correlations decay more slowly and new dynamical effects come into play. Since this phenomenon alters the statistical properties of the motion across the stochastic layer, it is expected to affect the rate of modulational (i.e. longitudinal) diffusion as well. We recall that two different asymptotic regimes are possible, depending whether λ or the product $\lambda\Omega$ are kept constant while taking the limit Ω (or V) $\rightarrow 0$ (cf. section 2). Accordingly, we shall discriminate among these two possibilities also in the case of modulational diffusion.

In the case $\Omega \rightarrow 0$ with $\lambda = \text{const.}$, the layer is progressively transformed into a thin separatrix layer. As a result, the modulational diffusion is converted into the weaker Arnold diffusion.

The other regime to be considered corresponds to $\Omega \rightarrow 0$ but $\lambda\Omega = \text{const.}$ (see section 2). The behaviour of the diffusion coefficient is unknown in this case, and this problem requires further investigation. However, preliminary numerical experiments indicate that within the range $0.1 < V < 1$, the diffusion rate does not differ considerably from that of the case $V > 1$. This result is consistent with the fact that the parameter V was not explicitly involved in the derivation of the diffusion coefficient.

A transition to a different diffusion regime will also occur when the overlap condition no longer holds. For $s < s_{\text{crit}}$ the layer decomposes into sublayers, due to the appearance of KAM surfaces within it. The theory developed in section 4 can be

generalized to this case from the following considerations.

The I_0 average in (3.11) must be restricted to a suitably smaller domain, corresponding to the sublayer to which the orbit belongs. In addition we recall that the resonant terms considered so far are effective only near the right boundary of the layer (see fig. 1). However, if a trajectory is confined to a sublayer located, say, near the left side of the layer, other terms become dominant and must be taken into account. We shall therefore consider also resonant lines of negative slope, corresponding to negative values of the index $J = \sum_k j_k$ (cf. (3.9) and (4.1)). By generalizing the procedure described in section 4, one can then identify dominant contribution and hence construct a complete map of the interaction regions, as depicted in fig. 7. The numbers labelling the regions in which the

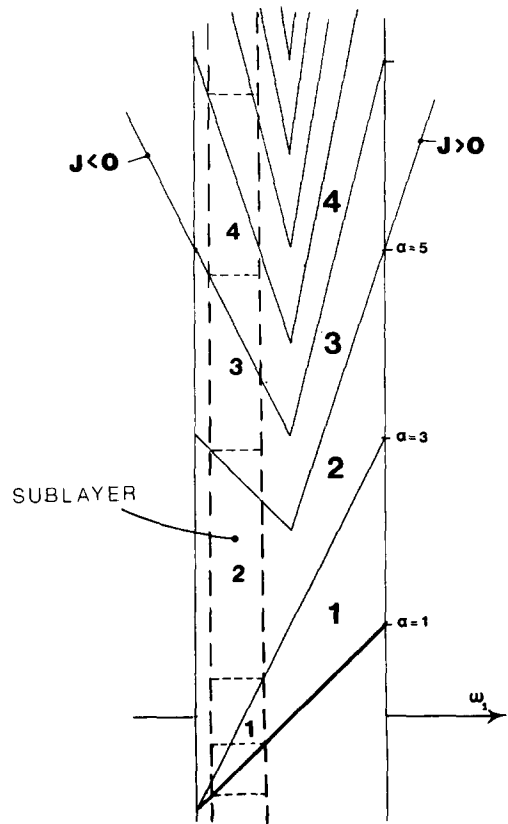


Fig. 7. Sublayer diffusion: map of interaction regions ($q = 1$).

layer decomposes denote the order of the perturbation parameter ϵ which characterizes the associated amplitudes. As an example, let us consider a sublayer as depicted in fig. 7, whose boundaries are represented by vertical dashed lines. The size of the corresponding plateaus varies with α , to attain an asymptotic value for large α . Since the latter is smaller than that corresponding to diffusion along the whole modulational layer, we expect the asymptotic parameters B and C corresponding to sublayer diffusion (cf. (6.2-3)) to be smaller. In particular the global decay rate B will be scaled as follows:

$$B \rightarrow B \left(2 - \frac{\max |I_0|}{\Delta\omega} \right), \tag{7.1}$$

where the maximum in (7.1) is taken over the sublayer domain.

The picture we have presented here will hold for sublayers whose size is larger than the resonance spacings. When this is no longer the case ($s \ll s_{\text{crit}}$), modulational sublayers are transformed into thin layers about separatrices of the multiplet resonances, and a transition to Arnold diffusion will occur.

In closing we would like to mention that the fine structure of the diffusion coefficient is actually much more complicated than that we have described so far. Indeed accurate numerical calculations have revealed a sharp increase in the diffusion rate about those values of α which correspond to integer and half-integer multiples of the

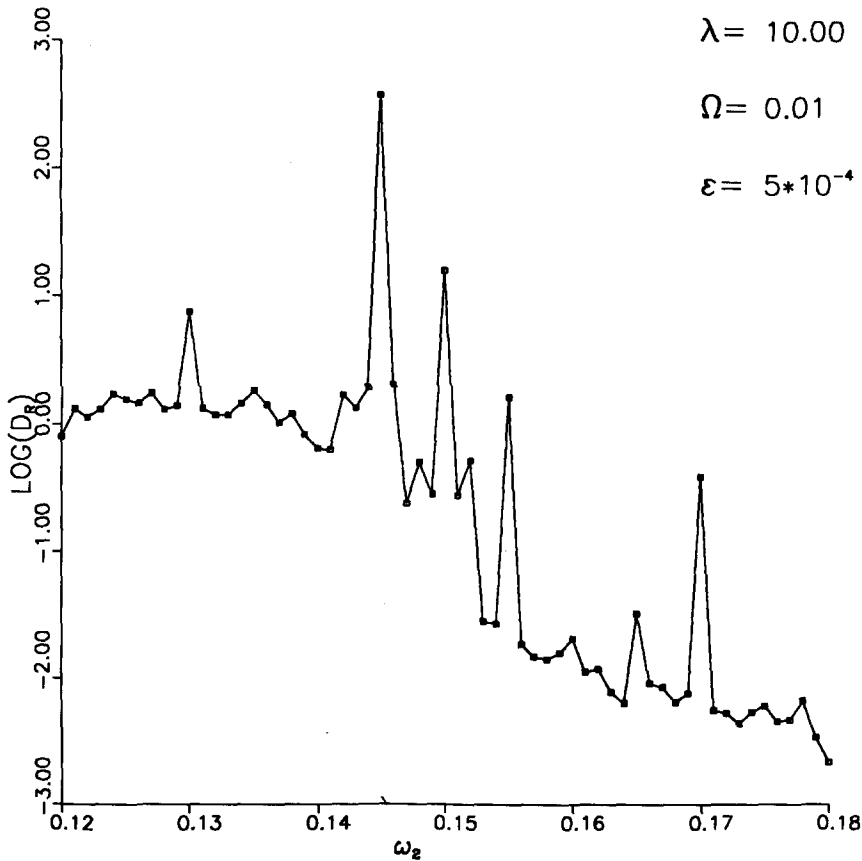


Fig. 8. Critical values of the detune ω_2 .

modulational frequency. In fig. 8 we display a fine scanning of such frequency in a domain centered on the precipice of the main plateau (for the unmodulated case), which uncovers variation in the diffusion rate up to three orders of magnitude. This phenomenon, which is currently under investigation, could originate from the “sticking” of phase points near the boundary of the modulational layer, which yields long segments of trajectories characterized by a very slow diffusive motion [15, 16].

Acknowledgements

This work was supported in part by DE-AS05-81ER4003, A001, and the U.S. National Science Foundation Grant ECS-8104561. Two of us (M.A.L. and F.M.V.) gratefully acknowledge the hospitality of the Aspen Center for Physics, where part of this work was carried out. We are also thankful to the unknown referees for their valuable comments which helped to improve the paper.

References

- [1] H. Poincaré, *Les Méthodes Nouvelles de la Mécanique Céleste* (Gauthier-Villars, Paris, 1892) NASA Translation TT-F450, Washington (1976).
- [2] V.I. Arnold, *Dokl. Akad. Nauk SSSR* 156 (1964) 9.
- [3] G.V. Gadiyak, F.M. Izrailev and B.V. Chirikov, *Proc. 7th Intl. Conf. On Nonlinear Oscillations*, (Berlin 1975), Vol. 2, p. 315.
- [4] B.V. Chirikov, *Physics Reports* 52 (1979) 263.
- [5] J. Tennyson, M.A. Lieberman and A. J. Lichtenberg, “Diffusion in Near-Integrable Hamiltonian Systems with Three Degrees of Freedom”, *A.I.P. Conf. Proc. no. 57* (A.I.P., New York, 1979), p. 272.
- [6] B.V. Chirikov, J. Ford and F. Vivaldi, “Some Numerical Studies of Arnold Diffusion in a Simple Model”, *A.I.P. Conf. Proc. no. 57* (A.I.P., New York, 1979), p. 324.
- [7] A.J. Lichtenberg and M.A. Lieberman, *Regular and Stochastic Motion* (Springer, New York, 1983).
- [8] B.V. Chirikov, *Proc. Intl. Conf. on Plasma Physics*, (Nagoya, 1980), Vol. 2, p. 176.
- [9] B.V. Chirikov, F.M. Izrailev and D.L. Shepelyansky, *Soviet Scientific Reviews 2C* (1981) 209.
- [10] B.V. Chirikov, J. Ford, F.M. Izrailev, D.L. Shepelyansky and F. Vivaldi, “The Modulational Diffusion in Nonlinear Oscillator Systems”, in: *Proc. IX Intl. Conf. Nonlinear Oscillations*, Kiev, U.S.S.R. (1981); *Naukova Dumka* (1984), Vol. 2, p. 80 (in Russian).
- [11] F. Vivaldi, “Weak Instabilities in Many-Dimensional Hamiltonian Systems”, *Rev. Mod. Phys.* 56 (1984) 737.
- [12] V.I. Arnold, *Russian Mathematical Surveys* 18 (1973) 85.
- [13] J. Tennyson, “The Instability Threshold for Bunched Beams in Isabelle”, *A.I.P. Conf. Proc. no. 57* (A.I.P., New York, 1979), p. 158.
- [14] B.V. Chirikov and D.L. Shepelyansky, “Diffusion in a Multiple Crossing of a Nonlinear Resonance”, Preprint 80-211, Institute of Nuclear Physics, Novosibirsk, U.S.S.R. (1980); *Zhurn. Tekhn. Fiz.* (Russian Journal of Technical Physics) 52 (1982) 238.
- [15] B. V. Chirikov and D.L. Shepelyansky, “The Statistics of the Poincaré Recurrence and the Structure of the Stochastic Layer of a Nonlinear Resonance”, Preprint 81-69, Institute of Nuclear Physics, Novosibirsk, U.S.S.R. (1981), *PPPL Trans.* 133, Princeton (1983).
- [16] C.F. Karney, *Physica* 8D (1983) 360.